J|A|C|S ARTICLES

Published on Web 11/17/2010

Role of the Charge-Transfer State in the Electronic Absorption of Protonated Hydrocarbon Molecules

Ivan Alata,[†,§] Claude Dedonder,[†,‡] Michel Broquier,[†,‡] Ernesto Marceca,[||] and Christophe Jouvet*[,†,‡]

Centre Laser de l'Université Paris Sud (LUMAT FR 2764), Bât. 106, and Institut des Sciences Moléculaires d'Orsay, Bât. 210, Université Paris-Sud 11, 91405 Orsay Cedex, France, Atomic Energy Commission of Syria, P.O. Box 6091, Damascus, Syria, and INQUIMAE-FCEN, UBA, Ciudad Universitaria, 3er piso, Pab. II, 1428 Buenos Aires, Argentina

Received July 20, 2010; E-mail: christophe.jouvet@u-psud.fr

Abstract: The vibrationally resolved electronic spectra of isolated protonated polycyclic aromatic hydrocarbons (PAHs)—naphthalene, anthracene, and tetracene—have been recorded via neutral photofragment spectroscopy. The $S_1 \leftarrow S_0$ transitions are all in the visible region and do not show a monotonic red shift as a function of the molecular size, as observed for the neutral analogues. Comparison with *ab initio* calculations indicates that this behavior is due to the nature of the excited state, which has a pronounced charge-transfer character for protonated linear PAHs with an even number of aromatic rings.

Introduction

Very little is known about the structure, dynamics, and electronic properties of even simple isolated polyaromatic protonated AH^+ ions. Recent advances in the development of efficient ion sources, sensitive spectroscopic detection, and ion trapping techniques have allowed substantial progress in the characterization of the ground-state geometric structure of isolated and microsolvated AH^+ ions in the gas phase.[1−5]

We have recently started to investigate the electronic structure and excited-state properties of very simple protonated aromatic molecules to get some information on these species, which are present in various environments. Knowledge about their spectroscopy is a necessary step to detect these ions in, for instance, molecular interstellar clouds, planetary atmosphere, plasmas, or jet engine exhaust.

We have shown that the excited-state properties of these excited protonated molecules are not simple to predict. *Ab initio* calculations indicate that the excited states of protonated benzene probably undergo a very fast internal conversion[6] and should be very short-lived. Indeed, the excited-state optimization leads without barrier to a geometry in which the ground- and excited-state energies are degenerate, i.e., to a conical intersection. In the first excited states, the system looses its planar symmetry, and conical intersections with the ground state arise along out-of-plane bending coordinates. With such a potential energy surface, a very fast internal conversion is expected.

This seems to be substantiated by experimental results, since we have been able to record well-structured photofragmentation spectra for protonated molecules such as benzaldehyde[7] and naphthalene[8] but not for benzene.

Compared to their neutral analogues, the protonated molecules in their excited states seem to be shorter lived, as is the case for protonated aromatic amino acids.[9−11] This is particularly true in the case of tryptophan, where the excited-state lifetime is in the femtosecond domain for the protonated species and in the nanosecond domain for neutral tryptophan. In this particular case, the $S_1 \leftarrow S_0$ transition energy of the protonated ion is very similar to the transition energy of the neutral molecule.[11,12]

Recently we reported the first observation of the excitation spectrum of protonated benzene dimer.[13] The observed transition is around 450 nm, largely red-shifted in comparison with the neutral dimer transition. This transition is also strongly red-shifted with respect to the protonated benzene transition.[14] This strong red-shift is due to the charge-transfer character of the first excited state, where an electron of the highest π orbital

† Centre Laser de l'Université Paris Sud.
§ Atomic Energy Commission of Syria.
‡ Institut des Sciences Moléculaires d'Orsay.
|| INQUIMAE-FCEN,UBA, Ciudad Universitaria.

(1) Lorenz, U. J.; Solca, N.; Lemaire, J.; Maitre, P.; Dopfer, O. *Angew. Chem., Int. Ed.* **2007**, *46*, 6714–6716.
(2) Solca, N.; Dopfer, O. *Angew. Chem., Int. Ed.* **2002**, *41*, 3628–3631.
(3) Knorke, H.; Langer, J.; Oomens, J.; Dopfer, O. *Astrophys. J.* **2009**, *706*, L66–L70.
(4) Zhao, D.; Langer, J.; Oomens, J.; Dopfer, O. *J. Chem. Phys.* **2009**, *131*, 184307.
(5) Ricks, A. M.; Douberly, G. E.; Duncan, M. A. *Astrophys. J.* **2009**, *702*, 301–306.
(6) Rode, M. F.; Sobolewski, A. L.; Dedonder-Lardeux, C.; Jouvet, C.; Dopfer, O. *J. Phys. Chem. A* **2009**, *113*, 5865–5873.
(7) Alata, I.; Omidyan, R.; Dedonder-Lardeux, C.; Broquier, M.; Jouvet, C. *Phys. Chem. Chem. Phys.* **2009**, *11*, 11479–11486.
(8) Alata, I.; Omidyan, R.; Broquier, M.; Dedonder, C.; Dopfer, O.; Jouvet, C. *Phys. Chem. Chem. Phys.* **2010**, *12*, 14456–14458.
(9) Kang, H.; Jouvet, C.; Dedonder-Lardeux, C.; Martrenchard, S.; Gregoire, G.; Desfrancois, C.; Schermann, J. P.; Barat, M.; Fayeton, J. A. *Phys. Chem. Chem. Phys.* **2005**, *7*, 394–398.
(10) Gregoire, G.; Jouvet, C.; Dedonder, C.; Sobolewski, A. L. *Chem. Phys.* **2006**, *324*, 398–404.
(11) Boyarkin, O. V.; Mercier, S. R.; Kamariotis, A.; Rizzo, T. R. *J. Am. Chem. Soc.* **2006**, *128*, 2816–2817.
(12) Rizzo, T. R.; Stearns, J. A.; Boyarkin, O. V. *Int. Rev. Phys. Chem.* **2009**, *28*, 481–515.
(13) Chakraborty, S.; Omidyan, R.; Alata, I.; Nielsen, I. B.; Dedonder, C.; Broquier, M.; Jouvet, C. *J. Am. Chem. Soc.* **2009**, *131*, 11091–11097.
(14) Freiser, B. S.; Beauchamp, J. L. *J. Am. Chem. Soc.* **1976**, *98*, 3136–3139.

localized on the neutral benzene moiety is transferred to a π^* orbital localized on the protonated benzene part.

In the present paper, we address the following questions on simple protonated aromatic molecules, the linear polycyclic aromatic hydrocarbons (PAHs):

(1) In neutral PAHs, the electronic absorption energy scales with the number of the aromatic cycles. This can be interpreted in terms of the simple "particle in a box" picture, where the larger the box containing the delocalized electrons, the smaller the energy gap between the quantum states. Is this also valid for the protonated species?

(2) What is the excited-state lifetime of protonated PAHs? There is an intrinsic relation between the excited-state geometry change and the excited-state lifetime. Indeed, large geometry changes lead quite often to conical intersections with the ground state and thus to very short lifetimes, as, for example, in DNA bases.[15,16] This is also the case for protonated benzene, in which calculations predict a conical intersection between S_1 and S_0, and the spectrum shows no vibrational structure because the excited-state lifetime is expected to be very short. In contrast, in protonated naphthalene, the ground- and excited-state geometries are more similar, and vibrationally resolved photofragmentation spectra have been obtained.[8] What will be the case for larger protonated PAHs?

(3) What is the nature of the excited state? In the protonated benzene dimer and in protonated naphthalene, the excited state has a strong charge-transfer character. Is this also true for larger PAHs?

We present the experimental excitation spectra of protonated linear PAHs anthracene and tetracene that will be compared to the spectrum of protonated naphthalene. As we will see, the non-monotonic shift of the first electronic transition with the number of aromatic cycles can be understood by considering the character of the excited states (charge-transfer state or not), evidenced through *ab initio* calculations. For protonated naphthalene and anthracene, a vibrational analysis has been performed, and a good agreement between calculated and experimental spectra is obtained.

Experimental Section

The experimental setup used to collect the electronic absorption spectra of protonated PAHs is depicted in Figure 1. The apparatus has been described previously[8,13] in detail (see also the Supporting Information). Here, we present a brief summary of the main components and give a short explanation of the spectroscopic method. Protonated PAH ions are produced by a synchronized discharge, ignited in a pulsed supersonic expansion of a 1:1 H_2-He gaseous mixture at a pressure of about 2 bar. The temperature of the expansion/discharge source assembly, adapted from the valve design by Ebata et al.,[17] was adjusted according to the volatility of the different PAHs, being always $T < 250$ °C.

Jet-cooled protonated MH^+ ions (as well as $M^{+\bullet}$ radical cations) that emerge from the source are extracted and accelerated in a reflectron time-of-flight (TOF) mass spectrometer. The mass resolution of the instrument in the linear configuration is better than one mass unit; this allows us to perform fragmentation spectroscopy measurements on the protonated species even when radical cations are also present in the beam. A large proportion of H_2 in the expansion mixture was found to increment the concentration of the protonated species in the beam, being on average about 10 times larger than that corresponding to the radical cation.

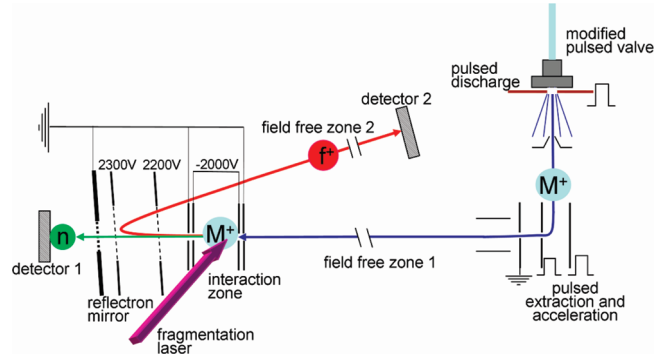

Figure 1. Scheme of the experimental setup. The ions are formed in an electric discharge located just after the pulsed valve generating the supersonic expansion. The jet is skimmed, and the ions are extracted and accelerated with pulsed voltages and enter a first field-free region. They enter the interaction zone located just in front of the electrostatic reflector, where they are photofragmented with the laser. The ions are selected by their arrival time in the interaction region. The interaction zone is held at a fixed potential so that the neutral fragments have a sufficient kinetic energy to be detected efficiently on detector 1 and differentiated from collision-induced fragments. The unfragmented parent ions as well as the fragment ions are reflected and may be detected after the second field-free region on a second microchannel plate detector 2.

At the end of the field-free zone 1, mass-selected ions are resonantly photofragmented inside an interaction region (see Figure 1), where they are intersected by an optical parametric oscillator laser. This is achieved by properly adjusting the delay between ion extraction and firing of the laser pulse. The potential of the interaction region is held at −2000 V, because in this way the kinetic energy gained by the ions is high enough to ensure that the photogenerated neutrals will be detected by the multichannel plate detector 1. It also allows discriminating neutrals coming from photofragmentation from neutrals due to collision-induced dissociation in the field-free zone. Conversely, all the ions (parents and daughter ions) will bounce in the reflectron mirror and fly across the field-free zone 2 toward detector 2. Photofragmentation spectra such as those shown in Figure 2 are obtained by plotting the neutrals signal measured at detector 1 *vs* the excitation wavelength.

Since our detection relies on the fragmentation of the molecule, the first band in the electronic spectrum may correspond to the fragmentation threshold. If this were the case, one should observe a rather long fragmentation time for the first band and a strong dependence of the fragmentation time on the excess energy. The fragmentation time can be measured when a 1 kV/cm electric field is applied in the interaction zone. Under these conditions, the kinetic energy of the parent ion will decrease as it travels inside the interaction zone, and the neutral fragment emitted will keep its parent ion velocity. As a result, if the fragmentation time is longer than 10 ns (the time resolution achieved by this technique),[18] the signal collected on detector 1 will give rise to a broad, slow-decaying TOF peak corresponding to neutrals emitted in the course of the parent ion lifetime. Such a broadening was not observed in the present experiment upon excitation on the first absorption band, implying that the observed spectra do not correspond to a fragmentation process at threshold but to a multiphoton absorption mechanism.

The real difficulty of this experiment concerns the generation of cold protonated ions. On one hand, a large number of collisions with the seeding gas will be necessary to cool down the PAH molecules vaporized in the source oven and further heated by the protonation process (probably due to the reaction with H_3^+ produced

(15) Perun, S.; Sobolewski, A. L.; Domcke, W. *J. Am. Chem. Soc.* **2005**, *127*, 6257–6265.
(16) Perun, S.; Sobolewski, A. L.; Domcke, W. *J. Phys. Chem. A* **2006**, *110*, 9031–9038.
(17) Ebata, T. *Bull. Chem. Soc. Jpn.* **2009**, *82*, 127–151.
(18) Lucas, B.; Barat, B.; Fayeton, J. A.; Jouvet, C.; Çarçabal, P.; Grégoire, G. *Chem. Phys.* **2008**, *347*, 324–330.

by the discharge). On the other hand, if there are too many collisions, the amount of ions might decrease by recombination with the electrons present in the plasma generated in the discharge. Hence, a careful optimization of the source conditions is required to maximize the formation of cold species in the beam. All the recorded spectra exhibit vibrational bands of protonated PAH ions superimposed on a continuous background. We have assigned this background signal to hot molecules left over after the cooling process, meaning that probably only a small portion of the protonated ions produced in the discharge contributes to the structured spectrum. As a consequence, cold protonated ions of larger PAHs will be more difficult to generate because a higher source temperature must be used as a result of their lower vapor pressures, increasing the initial internal energy of the precursor ions that will be more difficult to cool down.

Calculations

Ab initio calculations have been performed with the TURBOMOLE program package,[19] making use of the resolution-of-the-identity (RI) approximation for the evaluation of the electron-repulsion integrals. The equilibrium geometry of the ground electronic state (S_0) has been determined at the MP2 level. Excitation energies and equilibrium geometry of the lowest excited singlet state (S_1) have been determined at the RI-CC2 level. Calculations were performed with the SVP basis set (7s4p1d for carbon and 4s1p for hydrogen)[20] because of the size of the molecules. To test the error induced by the limited size of the basis set, a larger correlation-consistent basis set[21] (cc-pVDZ, 17s4p1d for carbon and 4s1p for hydrogen)[22] was used to calculate the transition energy of protonated naphthalene.

A complete vibrational analysis has been performed for the two smallest molecules, protonated naphthalene and anthracene: after the excited-state optimization, the vibrational frequencies were calculated in both the ground and excited states, and then a Franck−Condon analysis was performed using the Pgopher software.[23]

Results and Discussion

a. Experiment. In Figure 2 are presented the photofragmentation spectra of protonated naphthalene, anthracene, and tetracene. As discussed above, the spectra are composed of sharp vibrational bands issued from cold molecules superimposed on a background issued from hot molecules. Protonated naphthalene and anthracene absorb in the same spectral region, whereas protonated tetracene is strongly red-shifted. The spectra start at 503.36 nm for protonated naphthalene, 491.43 nm for protonated anthracene, and 679.90 nm for protonated tetracene, with an accuracy of ~3 cm^{-1} (0.1 nm). It should be noticed that the photofragmentation spectrum obtained for protonated anthracene presents sharper vibronic structures than the photofragmentation spectrum of its complex with water recorded by V.A. Kapinus.[24]

As already mentioned, the first band observed in the spectra may correspond to the dissociation threshold. However, when a 1 kV/cm electric field is applied in the interaction region, there is no broadening of the photofragment peak, indicating that the neutrals are produced in a few tens of nanoseconds for the first band, which seems too short for a fragmentation at threshold.

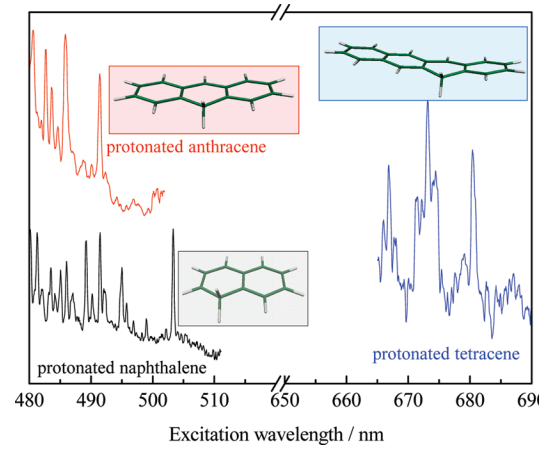

Figure 2. Photofragmentation spectra of protonated linear PAHs. The intensities have been normalized to the first band in each spectrum. The excited-state geometries of the protonated molecules are represented in the insets.

The dissociation threshold for protonated naphthalene has been calculated at 2.69 eV,[1] and for protonated anthracene and tetracene, assuming that the main dissociation path is the loss of atomic hydrogen as in IRMPD,[3] the dissociation energy can be evaluated from the thermochemical data[25] as

$$E_{diss}(MH^+ \rightarrow M^+ + H) = PA(M) + IP(M) - IP(H)$$

where PA(M) is the proton affinity of the neutral molecule M, IP(M) is its ionization energy, and IP(H) is the ionization potential of the hydrogen atom. This estimation leads to dissociation values of 2.93 eV for anthracene and 2.75 eV for tetracene. In all these cases, the first bands observed in the spectra lie below the dissociation threshold. The spectrum is thus not limited by the fragmentation threshold at low energy, and the dissociation is a multiphoton process via the resonant $S_1 \leftarrow S_0$ transition.

In a first step we will consider that the first band observed in each spectrum corresponds to the 0−0 transition. Under this hypothesis, the strong 0−0 transitions observed imply that the excited-state equilibrium geometry is not strongly changed as compared to the ground-state geometry, in contrast to the benzene case, for which the geometry change is predicted to be very important.

In addition, we have estimated that the excited-state lifetimes are not very short, i.e., longer than ~1 ps, in contrast to protonated benzene or tryptophan, since the bandwidths, including the rotational envelope, are on the order of 10 cm^{-1}.

b. Calculations. For each system, we searched for the most stable isomer in the ground state at the RI-MP2 level. The isomers calculated are presented in Figure 3. The ground-state energies of the different isomers are given in Table 1, the energy being referenced to the most stable isomer. This most stable structure corresponds to the isomer for which the proton is located closer to the middle of the PAH chain, as in previous DFT calculations.[3,24]

Only the most stable isomer of protonated pentacene, with the proton attached to the central ring, has been calculated.

(19) Turbomole V6.1, 2009, a development of the University of Karlsruhe and Forschungazentrum Karlsruhe GmbH, 1989−2007, Turbomole GmbH, since 2007; available from http://www.turbomole.com.
(20) Schäfer, A.; Horn, H.; Ahlrichs, R. *J. Chem. Phys.* **1992**, *97*, 2571–2577.
(21) Dunning, T. H. *J. Chem. Phys.* **1989**, *90*, 1007–1023.
(22) Weigend, F.; Köhn, A; Hättig, C. *J. Chem. Phys.* **2002**, *116*, 3175–3183.
(23) Western, C. M. A Program for Simulating Rotational Structure, University of Bristol, http://pgopher.chm.bris.ac.uk.
(24) Kapinus, V. A. Photophysical Properties of Protonated Aromatic Hydrocarbons. http://www.gps.caltech.edu/~gab/publications/gabtheses/vadym_thesis.pdf.
(25) NIST Webbook of chemistry, http://webbook.nist.gov/chemistry/.

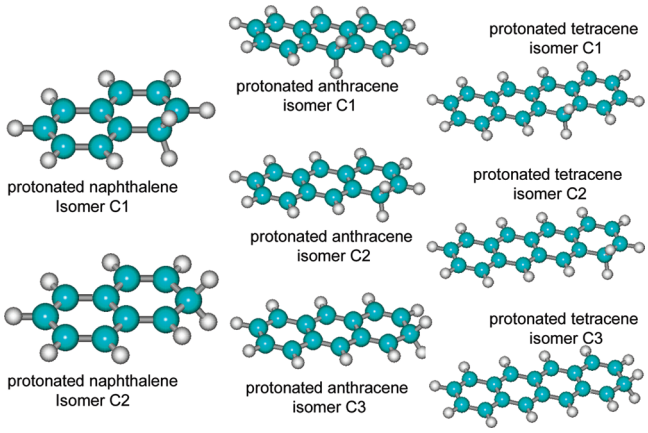

Figure 3. Different isomers calculated for protonated naphthalene, anthracene, and tetracene.

Table 1. Ground- and Excited-State Energies for Protonated Naphthalene, Anthracene and Tetracene Calculated at the RI-MP2/RI-CC2 (SVP) Level[a]

	ground-state energy/C1[b]	S_1 vertical transition energy[c]	S_2 vertical transition energy[c]	$S_1 \leftarrow S_0$ adiabatic transition energy[d]
		NaphthaleneH$^+$ (obs = 2.47 eV)		
C1	0	3.0	3.5	2.6 (2.5 ZPE corrected)
C2	0.15/0.16	2.8	4.5	2.5 (2.4 ZPE corrected)
		AnthraceneH$^+$ (obs = 2.51 eV)		
C1	0	2.9	3.2	2.7 (2.5 ZPE corrected)
C2	0.45	2.0	5.0	1.7
C3	0.61	1.9	5.0	1.6
		TetraceneH$^+$ (obs = 1.82 eV)		
C1	0	2.2	3.0	1.9
C2	0.64	1.5	2.9	1.2
C3	0.79	1.4	2.9	1.1
		PentaceneH$^+$ [e]		
C1	0	2.1	2.3	2.0

[a] All the values are given in eV. [b] Ground-state energy for the different isomers. The energies are referenced to the most stable C1 isomer, which is the one where the proton is closest to the middle of the PAH chain (see Figure 3). Absolute ground-state energies in hartrees: naphthalene, SCF energy = −383.400993521, final MP2 energy = −384.675988538; anthracene, SCF energy = −535.960776437, final MP2 energy = −537.747808318; tetracene, SCF energy = −688.501521449, final MP2 energy = −690.802582640; pentacene, SCF energy = −841.040692437, final MP2 energy = −843.858554987. [c] Vertical excitation energies (S_1 and S_2 energies at the ground-state geometry). [d] Calculated adiabatic transition: S_1 energy (after optimization of the S_1 geometry) minus S_0 energy (after S_0 optimization). This value corresponds to the transition energy and can be compared with the experimental band origin (obs) given in the headings. [e] For pentacene, only the most stable C1 isomer with the proton on the central ring has been calculated for comparison with the smaller molecules.

For each isomer, the vertical and adiabatic transition energies have been calculated; the latter can be directly compared with the experimental spectrum, provided the structural changes between the ground and excited states are not too large so that the 0−0 transition will have a reasonable Franck−Condon factor.

For naphthalene and anthracene, the ground- and excited-state zero-point energies (ZPEs) have been calculated for the most stable isomer to correct the transition energy.

For naphthalene, the ground state retains a planar C_s symmetry, and the excited state presents a local minimum in planar C_s symmetry for the two isomers.

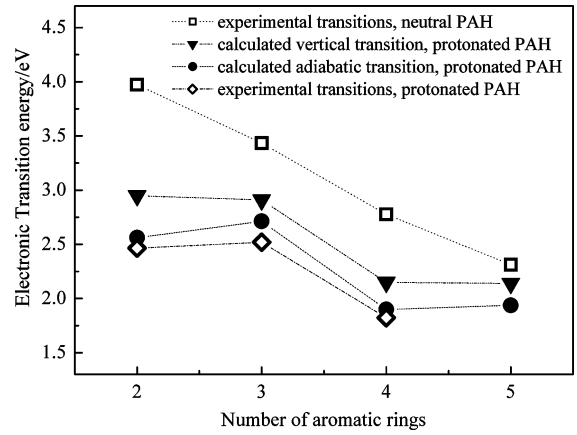

Figure 4. Variation of the first $S_1 \leftarrow S_0$ electronic transition of linear PAHs with the number of aromatic rings: □, experimental transitions of neutral PAHs;[26−29] ▲, calculated vertical transitions for protonated PAHs; ●, calculated adiabatic transitions for protonated PAHs; ◇, experimental band origins of protonated PAHs.

For anthracene and tetracene, the ground- and excited-state geometries deviate slightly from C_s symmetry, the carbon atom linked to 2 hydrogen atoms coming slightly out of the molecular plane by 10°.

For the most stable isomers, the calculations show that the changes in geometry between the ground and the first excited state are not very large, and Franck−Condon factors for the 0−0 transition can be expected to be reasonable. This corroborates the assignment of the first band observed in each spectrum to the 0−0 transition.

The values of the transition energies calculated and observed for the protonated molecules are displayed in Figure 4 as a function of the number of aromatic rings and compared with the transition energies of the neutral linear PAHs.[26−29]

Discussion

a. Comparison between Experiment and Calculated Transitions. As can be seen in Table 1, the agreement between the calculated adiabatic transition energy for the most stable isomers and the experiment is quite good, while the vertical transition energies do not agree with the experimental observations. This shows that the excited-state optimization is a necessary step to get reasonable agreement and that the RI-CC2 method gives reliable results at a reasonable computing cost for these systems. Note that single-configuration methods give a good description of the electronic states when the double-excitation character remains small,[30] which is the case for the molecules considered here, the single-excitation character being between 85 and 90%.

For the smaller systems (protonated naphthalene and anthracene), the agreement is even better when the variation of ZPE between the ground and excited states is taken into account. This requires the calculation of the S_1 and S_0 vibrational

(26) Cockett, M. C. R.; Ozeki, H.; Okuyama, K.; Kimura, K. *J. Chem. Phys.* **1993**, *98*, 7763–7772.
(27) Hoheisel, G.; Heinecke, E.; Hese, A. *Chem. Phys. Lett.* **2003**, *373*, 416–421.
(28) Lambert, W. R.; Felker, P. M.; Syage, J. A.; Zewail, A. H. *J. Chem. Phys.* **1984**, *81*, 2195–2208.
(29) Vanherpen, W. M.; Meerts, W. L.; Dymanus, A. *J. Chem. Phys.* **1987**, *87*, 182–190.
(30) Schreiber, M.; Silva-Junior, M.; Sauer, S.; Thiel, W. *J. Chem. Phys.* **2008**, *128*, 134110.

frequencies, and the δZPE values calculated are 0.12 eV for protonated naphthalene and 0.18 eV for protonated anthracene.

It should be noticed that very good agreement between the observed spectrum and the calculated adiabatic transition energy is obtained for the most stable isomer. For protonated anthracene and tetracene, the electronic transitions of the other isomers are shifted by more than 0.8 eV and cannot account for the observed spectra, which indicates that electronic spectroscopy can be useful to differentiate ground-state isomers.

In the case of protonated naphthalene, the calculated adiabatic transition energies for the two isomers are close. It seems, however, that we see only one isomer, and since the C1 isomer is the most stable[1,5,31] and the transition calculated with ZPE correction is very close to the experimental origin, while the transition energy for the C2 isomer is lower, we assign the observed spectrum to the C1 isomer.

One can wonder about the accuracy of these calculations. From the experimentalist point of view, the best criterion would be the comparison of calculations with experimental measurements, which requires at least the excited-state optimization that gives the adiabatic transition energy, red-shifted by typically 0.3 eV from the vertical transition energy, as can be seen in Table 1. For smaller molecules−neutral benzene derivatives (phenol, etc.) or other small protonated aromatic molecules−we have compared experimental and calculated transition energies for a set of 18 molecules using the RI-CC2 method with the cc-pVDZ or aug-cc-pVDZ basis set. The average error (experimental − calculated value) is −0.15 eV, without ZPE correction, with a standard deviation of 0.11 eV, the largest error being −0.4 eV.

The basis set effect has been investigated in the case of protonated naphthalene and is not very large, the adiabatic transition energy being 2.56 eV using the cc-pVDZ basis set,[22] 2.54 eV with the aug-cc-pVDZ basis set, and 2.61 eV for the smaller SVP basis set.

The ground states of protonated anthracene and tetracene are found nonplanar in the RI-MP2 (SVP) calculation, while these molecules stay planar in DFT calculations: there is clearly a method effect. However, in the case of protonated anthracene, for which one can compare the calculations with the experimental results (vibrational and electronic spectra), it seems that the calculations with a distorted structure give a better agreement with the experiment (see Vibrational Analysis below). The physical origin of this effect is still not clear. A possible reason may be that protonation giving a sp^3 character to the protonated carbon decreases the aromaticity of the molecule and induces out-of-plane deformations.

b. Comparison between Neutral and Protonated Molecules. The electronic structures of the neutral and protonated molecules are similar, both having a closed-shell structure and the same number of electrons, but their electronic spectra are quite different. For the neutral molecules, the electronic transition energies slowly decrease as the size of the molecules increases (Figure 4). In contrast, for the protonated ions, the transition energy does not show a monotonic behavior. The anthracene transition is blue-shifted as compared to the naphthalene transition, and the tetracene transition is red-shifted. This behavior can be understood on the basis of *ab initio* calculations.

In anthracene and pentacene, the lowest excited state corresponds to a transition from the HOMO−1 orbital toward the LUMO, and for naphthalene and tetracene, the lowest excited state involves a HOMO−LUMO transition. Figure 5 shows that, for an even number of aromatic rings, the excitation corresponds to the transition of an electron from the nonprotonated part of the molecule to the protonated part. This charge-transfer character is very similar to what has been observed for the benzene dimer, in which the lowest excited state corresponds to the excitation of the electron from the neutral benzene toward the protonated benzene part. The reason the charge transfer state is very low in energy in the case of the protonated benzene dimer can be understood with simple arguments: in a crude approximation, the HOMO−LUMO gap is not very different in the protonated and the neutral molecules. However, the HOMO orbital of protonated benzene is significantly lower in energy, because the positive charge increases the ionization energy due to larger Coulomb attraction. Thus, in the protonated benzene dimer, the HOMO is localized on the neutral benzene part, whereas the LUMO is localized on the protonated benzene moiety. Consequently, the HOMO−LUMO electronic transition corresponds to a charge-transfer state which is lower in energy than the transitions localized on each of the constituents. The charge-transfer state of protonated benzene dimer leads to an intense absorption observed in the visible region.[13] The situation is analogous in protonated naphthalene: the two parts of the molecule are no longer equivalent, and there is a charge transfer from the neutral aromatic ring to the protonated moiety, leading to a large red shift of the transition as compared to neutral naphthalene.[8] The results obtained for protonated tetracene indicate that this charge transfer also occurs in larger systems.

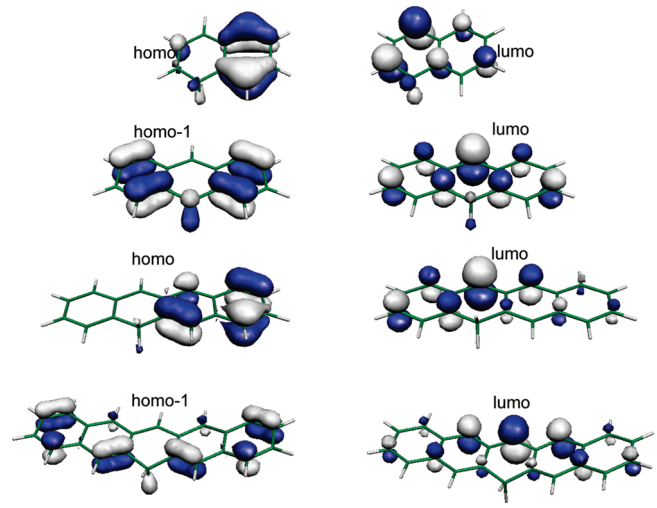

Figure 5. Orbitals involved in the excited-state transitions of protonated linear PAHs.

For molecules with an odd number of aromatic rings, in the most stable structure the proton is located on the central ring, with a symmetry plane perpendicular to the molecular rings and including the CH_2 group (C_s molecular symmetry). Under this symmetry, there is no charge-transfer state, and thus the excitation is more similar to the $\pi\pi^*$ excitation of the neutral molecules, which is higher in energy.

c. Vibrational Analysis. For the two smallest molecules, full vibrational analysis has been performed; i.e., both ground- and excited-state vibrations have been calculated, and simulated spectra have been generated. The vibrational modes are listed in the Supporting Information (Tables SI-1 and SI-2), as well as the corresponding geometries.

(31) Sebree, J. A.; Kislov, V. V.; Mebel, A. M.; Zwier, T. S. *J. Phys. Chem. A* **2010**, *114*, 6255–6262.

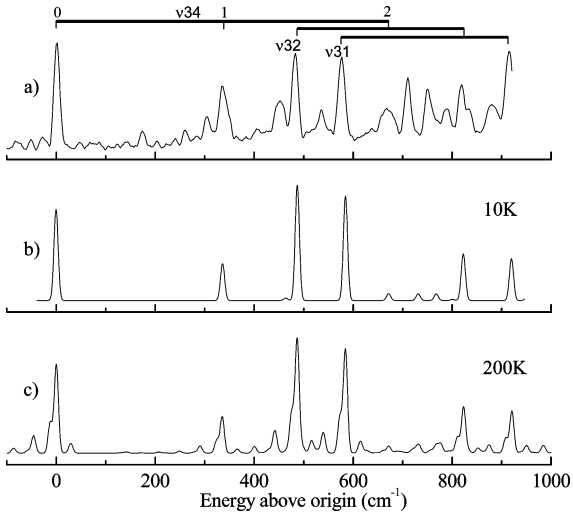

Figure 6. Comparison between experimental and calculated spectra for protonated naphthalene. The ground-state frequencies are calculated at the RI-MP2/cc-pVDZ level and the excited-state frequencies at the RI-CC2/cc-pVDZ level: (a) experimental spectrum; (b) simulated spectrum for a temperature of 10 K; (c) simulated spectrum for a temperature of 200 K.

In Figure 6 is presented a comparison between the experimental and calculated spectra, in the spectral region where the bands are well resolved for protonated naphthalene. The simulated spectrum has been calculated with the cc-pVDZ basis set, and the vibrational assignment is given in the Supporting Information (Table SI-2).

As can be seen, the calculated spectrum is in rather good agreement with the experimental one. Both the band intensities and the positions are well reproduced. Some bands of the experimental spectrum are not present in the spectrum simulated at 10 K but appear in the simulation at higher temperature; i.e., they are hot bands. This means that our molecules are not very cold, which is not too surprising considering the mechanism used to produce the ions. The hot bands can be assigned to a low-frequency out-of-plane vibration (50^1_1).

Three active modes are clearly identified: ν34 (335 cm^{-1}), ν32 (481 cm^{-1}), and ν31 (575 cm^{-1}) (see Supporting Information Table SI-2). For these modes, the error of the calculation is very small, less than 3%. The active mode ν34 is observed with one and two quanta and in combination with the other active modes and corresponds to the opening of the central CC(H2)C angle, which is one of the coordinates that changes the most upon electronic excitation. The modes at 481 and 575 cm^{-1} also correspond to in-plane deformations of the carbon skeleton.

For protonated anthracene, simulated spectra have been obtained from *ab initio* calculations with two methods, DFT/TD-DFT (B3-LYP functional, SVP basis set) and RI-MP2/RI-CC2 (SVP). Using the DFT/TD-DFT method, both the ground and excited states stay planar, while the RI-MP2/RI-CC2 method gives nonplanar structures. Comparison with the experimental spectrum can help to test which method gives the best result.

The spectra simulated with the two methods are presented in Figure 7, and both compare quite nicely with the experimental spectrum.

Basically, the DFT/TD-DFT and RI-MP2/RI-CC2 simulated spectra are built on long progressions of the 232 cm^{-1} mode, which corresponds to the opening of the central CCC angle, alone or in combination with a mode at 371 cm^{-1} (see Supporting Information). In addition, some weaker modes are active in the RI-MP2/RI-CC2 spectrum which seem to be present in the experimental spectrum with a higher intensity. This observation seems to confirm that the planar symmetry is broken in protonated anthracene. It would be interesting to see

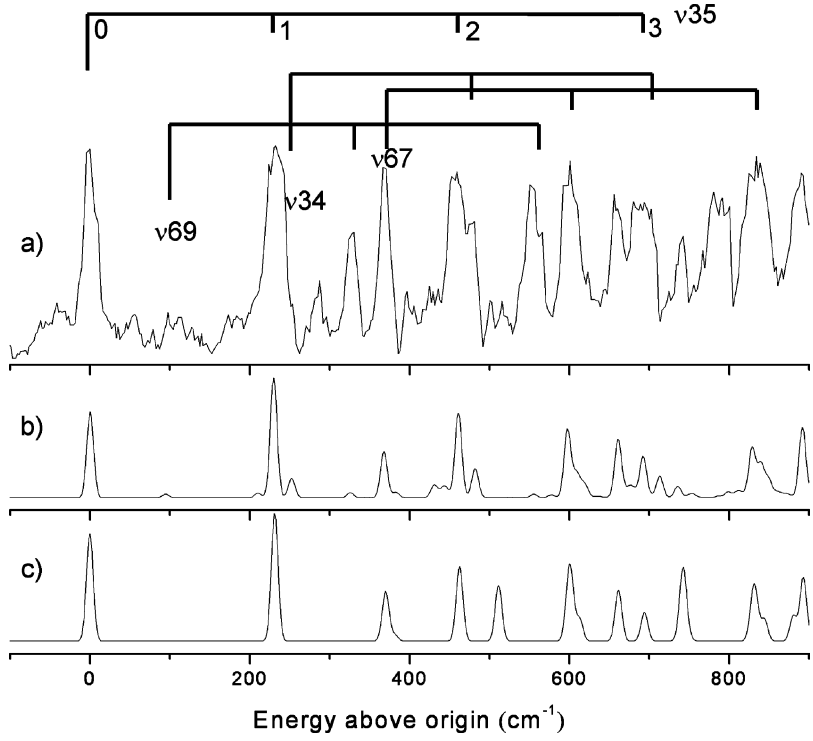

Figure 7. Comparison between experimental and calculated spectra for protonated anthracene. The ground- and excited-state frequencies are calculated with the SVP basis set: (a) experimental spectrum; (b) simulated spectrum using the RI-MP2/RI-CC2 method, where the molecule is nonplanar; (c) simulated spectrum with the DFT/TDDFT(B3LYP) method, where the molecule stays planar.

if other methods, in particular multireference methods, can confirm this nonplanar structure for protonated anthracene.

Interestingly, the most active modes in protonated anthracene are also active in the neutral molecule, although the geometry change of the protonated molecule upon excitation is much larger than for the neutral molecule,[28] which is reflected in the relative intensity of the 0−0 transition that is no longer the most intense vibrational band in the protonated molecule.

For tetracene, only the ground-state vibrations have been calculated. The experimental spectrum shows two vibronic bands at 160 and 300 cm^{-1} that can be tentatively assigned to vibrational modes similar to those active in the protonated anthracene spectrum: the mode calculated at 154 cm^{-1} in the ground state of tetracene corresponds to the opening of the central CCC angle and is equivalent to the mode at 232 cm^{-1} observed in protonated anthracene (and to mode 34 at 335 cm^{-1} in protonated naphthalene), and the mode calculated at 303 cm^{-1}, corresponding to a deformation of the carbon skeleton, is equivalent to the mode at 371 cm^{-1} in protonated anthracene and to mode 32 at 481 cm^{-1} in protonated naphthalene (see Supporting Information for a scheme of the vibrational modes).

d. Linear Protonated PAHs and Diffuse Interstellar Bands. Protonated PAHs have been suggested to be among the potential candidates for diffuse interstellar band (DIB) carriers.[32−35] If smaller $(PAH)H^+$ molecules are usually considered to be less favorable candidates, following photochemical stability arguments, larger ones may have a chance to be stable. It seems that there is no correspondence between the reported DIBs[36] and the bands observed in the present experiment. Thus, protonated naphthalene, anthracene, and tetracene are not among the most intense DIB carriers. Obviously, optical spectra of larger protonated PAHs ions are needed for testing the DIBs hypothesis, and corresponding experiments are currently underway.

Finally, the quality of comparison between calculations and experiment allows predicting that the pentacene transition should be higher in energy than that of tetracene. It has not yet been possible to confirm this prediction, since it seems very difficult to cool down this molecule. In the future we will test this prediction with an improved experimental setup.

Another point that will be addressed in the future is the properties of protonated nonlinear PAHs, which might be carriers of the DIBs.

Conclusions

We present the first experimental observation of vibrationally resolved electronic spectra of protonated linear PAHs. In contrast to the neutral molecules, the first electronic transitions are all in the visible region. The transition energies do not decrease monotonically with the size of the molecule as for their neutral counterparts, which may be understood with the help of *ab initio* calculations by the presence of low-lying charge-transfer states in the protonated PAHs with an even number of aromatic rings.

Acknowledgment. The authors thank Prof. O. Dopfer for helpful discussion. This work has been supported by the Université Paris-Sud 11, the ANR research grant (NT05-1 44224), and the PROCOPE 17832NK program. I.A. thanks the Atomic Energy Commission of Syria (http://www.aec.org.sy/) for financial support.

Supporting Information Available: Experimental setup and procedures, ground- and excited-state geometries and vibrational modes, and assignment of the spectra for protonated naphthalene and anthracene. This material is available free of charge via the Internet at http://pubs.acs.org.

JA106424F

(32) Le Page, V.; Keheyan, Y.; Bierbaum, V. M.; Snow, T. P. *J. Am. Chem. Soc.* **1997**, *119*, 8373–8374.
(33) Snow, T.; Page, L. V.; Keheyan, Y.; Bierbaum, V. M. *Nature* **1998**, *391*, 259–260.
(34) Pathak, A.; Sarre, P. J. *Monatsch. Not. R. Astron. Soc.: Lett.* **2008**, *391*, L10–L14.
(35) Hammonds, M.; Pathak, A.; Sarre, P. J. *Phys. Chem. Chem. Phys.* **2009**, *11*, 4458–4464.
(36) Jenniskens, P.; Desert, F. X. *Astron. Astrophys. Suppl. Ser.* **1994**, *106*, 39–78.